

Lepton flavour universality tests at LHCb

S. REICHERT on behalf of the LHCb COLLABORATION

Technische Universität Dortmund - Dortmund, Germany

received 16 September 2017

Summary. — Over the past years, tensions between lepton flavour universality as predicted in the Standard Model and experimental measurements have been observed. Results of lepton flavour universality tests in $B^+ \rightarrow K^+\ell^+\ell^-$, $B^0 \rightarrow D^{*-}\tau^+\nu_\tau$ as well as in $W \rightarrow \ell\nu_\ell$ decays by the LHCb Collaboration are summarised in these proceedings.

1. – Introduction

In the Standard Model of particle physics, the couplings of the weak interaction to leptons are predicted to be universal, wherefore a violation of this so-called lepton flavour universality would be a clear sign of physics beyond the Standard Model. Lepton flavour universality has been probed not only by the B-factories but also by the LHCb Collaboration by studying theoretically clean observables. Over the past years, several tensions between Standard Model predictions and experimental measurements have been observed in $b \rightarrow s\ell\ell$ decays [1-6], which are sensitive to new scalar or vector particles such as models with leptoquarks [7] or models with Z' bosons [8]. By analysing processes involving tau leptons in the final state, models with enhanced couplings to the third lepton generation can be scrutinised.

2. – R_K

A stringent test of lepton flavour universality is the measurement of the ratio of the differential branching fractions of $B^+ \rightarrow K^+\ell^+\ell^-$ decays, R_K , in a given range of q^2

$$(1) \quad R_K = \frac{\int_{q_{\min}^2}^{q_{\max}^2} \frac{d\Gamma(B^+ \rightarrow K^+\mu^+\mu^-)}{dq^2} dq^2}{\int_{q_{\min}^2}^{q_{\max}^2} \frac{d\Gamma(B^+ \rightarrow K^+e^+e^-)}{dq^2} dq^2}.$$

The Standard Model prediction of R_K is 1.00030 with an uncertainty of $\Delta R_K = +3\%$ arising from QED corrections [9]. The LHCb Collaboration has measured R_K [1] in the theoretically preferred range $1 < q^2 < 6 \text{ GeV}^2$ as a double ratio

$$(2) \quad R_K = \frac{\mathcal{N}_{K^+\mu^+\mu^-} \mathcal{N}_{J/\Psi(e^+e^-)K^+} \varepsilon_{K^+e^+e^-} \varepsilon_{J/\Psi(\mu^+\mu^-)K^+}}{\mathcal{N}_{K^+e^+e^-} \mathcal{N}_{J/\Psi(\mu^+\mu^-)K^+} \varepsilon_{K^+\mu^+\mu^-} \varepsilon_{J/\Psi(e^+e^-)K^+}},$$

with respect to the normalisation channel $B^+ \rightarrow K^+ J/\Psi$, where the J/Ψ decays either to a di-muon or di-electron final state, to minimise the effect of systematic uncertainties. The efficiencies comprise effects from each step of the analysis. Overall, the efficiency to reconstruct, select and identify a muon is two times higher than for an electron. The R_K measurement is performed on the 3 fb^{-1} dataset recorded in 2011 (2012) at centre-of-mass energies of $\sqrt{s} = 7(8) \text{ TeV}$. The mass shape of the B meson candidate in the di-electron mode is found to be dependent on the number of bremsstrahlung photons associated to the electrons as well as the transverse momentum of the electrons and the detector occupancy, wherefore R_K is measured in categories depending on whether the event was triggered by the electron, kaon or any other particle in the event. The signal yields in the normalisation and signal channels are extracted from unbinned maximum likelihood fits to the invariant mass of the kaon and di-lepton pair. The results of these fits to the di-electron mode are illustrated in fig. 1.

In the non-resonant $B^+ \rightarrow K^+ \mu^+ \mu^-$ channel, 1126 ± 41 candidates are observed and the yields obtained in the different trigger categories of $B^+ \rightarrow K^+ e^+ e^-$ candidates as well as the corresponding values of R_K are given in table I, where the dominant systematic uncertainties arise from the mass shape of $B^+ \rightarrow K^+ e^+ e^-$ candidates and trigger efficiencies.

The combined results yield $R_K = 0.745^{+0.090}_{-0.074} \pm 0.036$, which corresponds to a 2.6σ deviation from the Standard Model prediction [9]. A comparison with previous

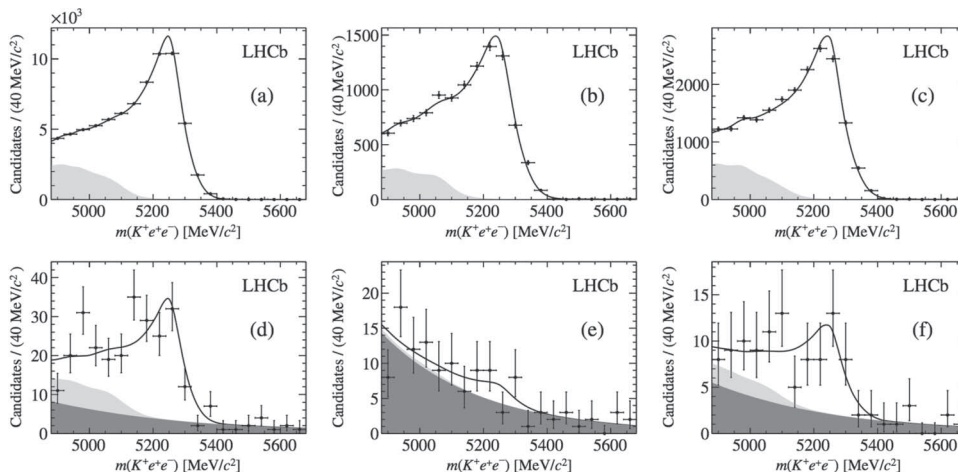


Fig. 1. – Mass distributions with fit projections overlaid of selected $B^+ \rightarrow K^+ J/\Psi(\rightarrow e^+ e^-)$ (top) and $B^+ \rightarrow K^+ e^+ e^-$ candidates (bottom). Figures (a) and (d) refer to candidates triggered by one of the two electrons, figs. (b) and (e) to candidates triggered by the kaon and figs. (c) and (f) to candidates triggered by any other particle in the event. Backgrounds from random combinations are illustrated in dark grey and from partially reconstructed decays in light grey.

TABLE I. – Signal yields of $B^+ \rightarrow K^+ e^+ e^-$ candidates triggered by one of the two electrons, kaon and any other particle in the event with the corresponding value of R_K . The uncertainties correspond to statistical and systematic uncertainties, respectively.

Triggered by	Electron	Kaon	Other
Yield	172^{+20}_{-19}	20^{+16}_{-14}	62 ± 13
R_K	$0.72^{+0.09}_{-0.08} \pm 0.04$	$1.84^{+1.15}_{-0.82} \pm 0.04$	$0.61^{+0.17}_{-0.07} \pm 0.04$

measurements from the B-factories is shown in fig. 2. The Belle Collaboration has published a measurement of R_K in the full q^2 range, $R_K^{\text{Belle}} = 1.03 \pm 0.19 \pm 0.06$ [10], whereas the BaBar Collaboration has studied the low and high q^2 regions, where R_K was found to be $R_K^{\text{BaBar}} = 0.74^{+0.40}_{-0.31} \pm 0.06$ and $R_K^{\text{BaBar}} = 1.43^{+0.65}_{-0.44} \pm 0.12$ [11], respectively. The measurements from the B-factories are compatible with the Standard Model prediction within less than one standard deviation.

3. – R_{D^*}

Beyond the Standard Model physics could appear not only in loops to which R_K is sensitive but also at tree level. The latter has been studied at LHCb with $\bar{B}^0 \rightarrow D^{*+} \tau^- \bar{\nu}_\tau$ decays [12] through the branching fraction ratio

$$(3) \quad R_{D^*} = \frac{\mathcal{B}(\bar{B}^0 \rightarrow D^{*+} \tau^- \bar{\nu}_\tau)}{\mathcal{B}(\bar{B}^0 \rightarrow D^{*+} \mu^- \bar{\nu}_\mu)},$$

which constitutes the first measurement of R_{D^*} at a hadron collider. In addition to the aforementioned hints of lepton flavour non-universality in R_K , the BaBar Collaboration had previously observed deviations from the Standard Model prediction [13] in R_{D^*} and the analogously defined R_D corresponding to a combined significance of 3.4σ [14], where

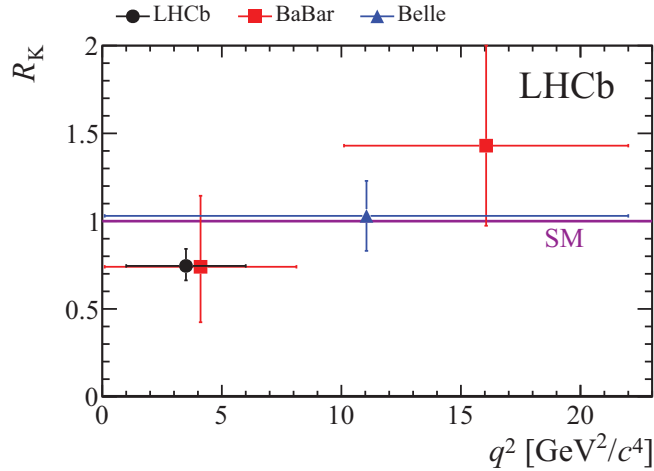


Fig. 2. – Comparison of R_K measurements in different ranges of q^2 from the LHCb Collaboration and the B-factories. For details, see text.

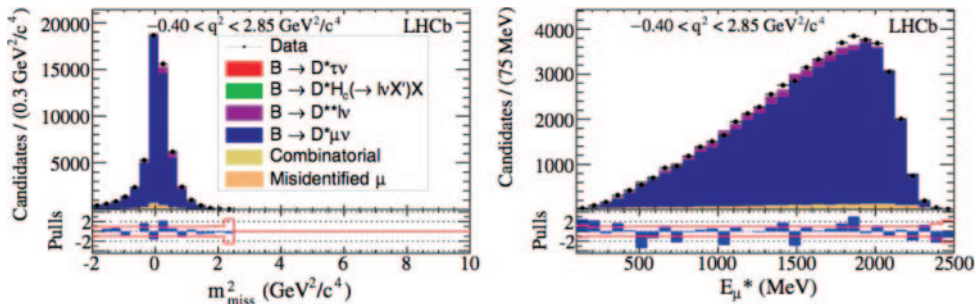


Fig. 3. – (Color online) Distributions of m_{miss}^2 (left) and E_{μ}^* (right) of selected candidates for various ranges of q^2 . The projections of the template fits are overlaid.

neutral as well as charged B meson decays were studied. In addition to muons, the BaBar measurement includes electrons in the final state of the signal and normalisation channels. In the LHCb analysis on the dataset of 3fb^{-1} recorded in 2011 and 2012, the decay $\bar{B}^0 \rightarrow D^{*+}\tau^-\bar{\nu}_{\tau}$ is reconstructed with $\tau^- \rightarrow \mu^-\bar{\nu}_{\mu}\nu_{\tau}$ decays, resulting in the same visible finale state for the signal and normalisation channel. Hence, the selection is chosen to preserve distinct kinematic features of the signal and normalisation channel caused by the mass difference between the τ and μ as well as the different numbers of neutrinos present in the final state. The most discriminating variables are the missing mass squared, m_{miss}^2 , the squared four-momentum transfer to the lepton system q^2 and the muon energy E_{μ}^* , which are computed in the rest frame of the B meson candidate. This approach relies on the estimation of the B meson candidate's momentum resulting in a sufficient resolution of 15–20% of the rest frame variables. The yields of the signal and normalisation channels are extracted from a binned maximum likelihood fit using three-dimensional templates in m_{miss}^2 , q^2 , E_{μ}^* for the signal, normalisation and background contributions, where the templates are derived from simulations. An exemplary fit projection in the q^2 range $-0.40 < q^2 < 2.85\text{GeV}^2$ is shown in fig. 3.

Dominant systematics arise from the template shape of background from misidentified muons and the simulated sample size as well as the trigger efficiencies. The uncorrected ratio of signal to normalisation channel yields amounts to $\mathcal{N}(\bar{B}^0 \rightarrow D^{*+}\tau^-\bar{\nu}_{\tau})/\mathcal{N}(\bar{B}^0 \rightarrow D^{*+}\mu^-\bar{\nu}_{\mu}) = (4.54 \pm 0.46)\%$, which results in $R_{D^*} = 0.336 \pm 0.027 \pm 0.030$, after accounting for efficiencies and $\mathcal{B}(\tau^- \rightarrow \mu^-\bar{\nu}_{\mu}\nu_{\tau})$. This measurement corresponds to a 2.1σ deviation from the Standard Model prediction [13], and deepens the tension observed by the BaBar Collaboration [14]. The result of the combination of various R_D and R_D^* measurements is illustrated in fig. 4 and exhibits a tension of 3.9σ between the combined average and the Standard Model prediction.

4. – $W \rightarrow \ell\nu$

A further test of lepton flavour universality on tree level processes is performed with $W \rightarrow \ell\nu$ decays utilised for a measurement of the forward production cross section [15] on the 2fb^{-1} dataset recorded in 2012 at $\sqrt{s} = 8\text{TeV}$. The combination of the two separate analyses of $W \rightarrow e\nu$ [15] and $W \rightarrow \mu\nu$ [16] allow to extract the ratio of branching fractions $\mathcal{B}(W \rightarrow e\nu)/\mathcal{B}(W \rightarrow \mu\nu)$ for both lepton charges and to compute an average.

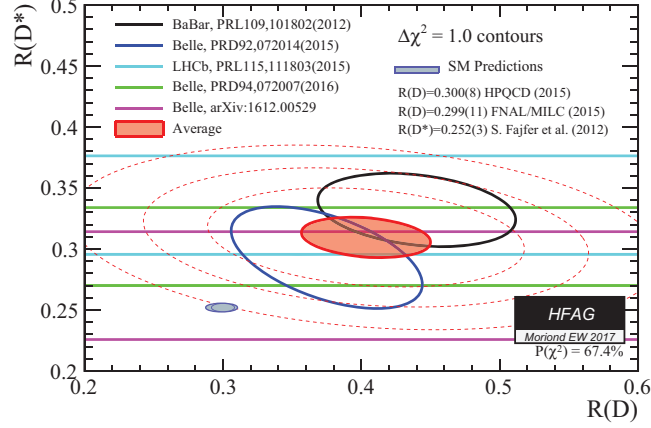


Fig. 4. – (Color online) Combination of R_D and R_D^* exhibiting a tension of 3.9σ with respect to the Standard Model predictions. Figure from [17].

The analysis strategy in both final states is similar: the cross section is measured in eight bins of pseudo-rapidity per lepton charge from a binned maximum likelihood template fit to the transverse momentum of the lepton. The templates are derived from simulations for the signal and for backgrounds from Z and W decays, $t\bar{t}$ production and decays in flight as well as from prompt $\gamma \rightarrow e^+e^-$ production relevant for the electron channel. Background templates for misidentified hadrons and heavy flavour decays are derived from data. Whenever possible, efficiencies are calculated from data or corrected with data-driven techniques. The fit to the electron p_T for the full dataset combining both electron charges is illustrated in fig. 5.

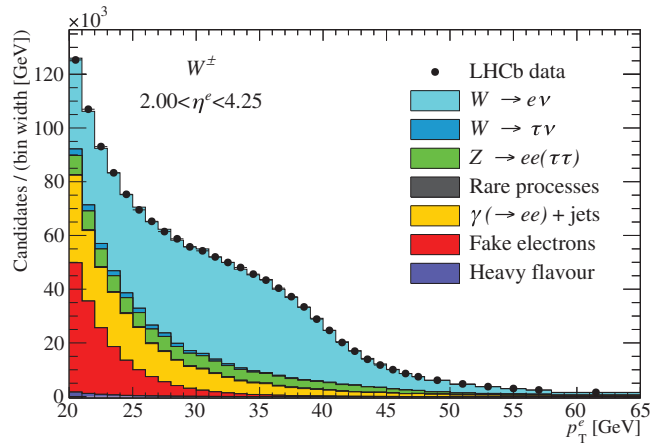


Fig. 5. – (Color online) Fit to the electron's transverse momentum distribution for the full dataset combining both electron charges.

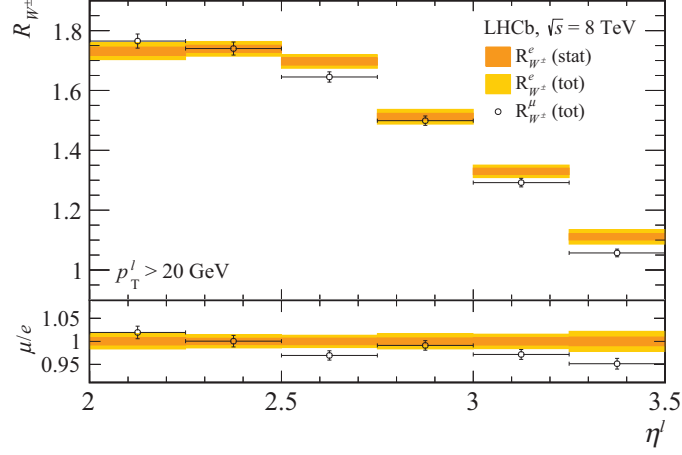


Fig. 6. – (Color online) The cross section ratio in bins of lepton pseudorapidity. The bottom panel displays the ratio of R_{W^\pm} obtained from the muon and electron final states.

The forward production cross sections are determined to be

$$(4a) \quad \sigma_{W^- \rightarrow e^- \bar{\nu}} = (809.0 \pm \pm 1.9 \pm 18.1 \pm 7.0 \pm 9.4) \text{pb},$$

$$(4b) \quad \sigma_{W^+ \rightarrow e^+ \nu} = (1124.4 \pm \pm 2.1 \pm 21.5 \pm 11.2 \pm 13.0) \text{pb},$$

$$(4c) \quad \sigma_{W^- \rightarrow \mu^- \bar{\nu}} = (818.4 \pm \pm 1.9 \pm 5.0 \pm 7.0 \pm 9.5) \text{pb},$$

$$(4d) \quad \sigma_{W^+ \rightarrow \mu^+ \nu} = (1093.6 \pm \pm 2.1 \pm 7.2 \pm 10.9 \pm 12.7) \text{pb},$$

where the uncertainties are statistical, systematic, from the LHC beam energy and the luminosity. The dominant systematic uncertainties arise from the templates and the efficiencies.

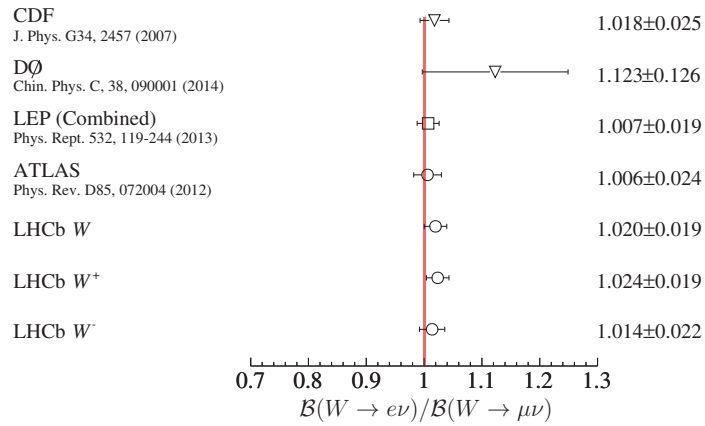


Fig. 7. – Comparison of the $\mathcal{B}(W \rightarrow e\nu)/\mathcal{B}(W \rightarrow \mu\nu)$ measurements. Details on the latest ATLAS measurement, which is not included in the comparison, can be found in the text.

No hint of a violation of lepton flavour universality is observed as is *e.g.* indicated by the W^+ to W^- production cross section ratio, R_{W^\pm} , illustrated in fig. 6. From the production cross sections, the ratio of branching fractions $\mathcal{B}(W \rightarrow e\nu)/\mathcal{B}(W \rightarrow \mu\nu)$ is computed. As the upper kinematic bounds in pseudorapidity η^ℓ differ for $W \rightarrow \mu\nu$ and $W \rightarrow e\nu$, the test of lepton flavour universality is restricted to $2.00 < \eta^\ell < 3.50$ and the ratios are found to be

$$(5a) \quad \frac{\mathcal{B}(W^+ \rightarrow e^+\nu_e)}{\mathcal{B}(W^+ \rightarrow \mu^+\nu_\mu)} = 1.024 \pm 0.003 \pm 0.019,$$

$$(5b) \quad \frac{\mathcal{B}(W^- \rightarrow e^-\bar{\nu}_e)}{\mathcal{B}(W^- \rightarrow \mu^-\bar{\nu}_\mu)} = 1.014 \pm 0.004 \pm 0.022,$$

$$(5c) \quad \frac{\mathcal{B}(W \rightarrow e\nu)}{\mathcal{B}(W \rightarrow \mu\nu)} = 1.020 \pm 0.002 \pm 0.019,$$

where the uncertainties are statistical and systematic. A comparison of the result with previous results is shown in fig. 7. The ATLAS Collaboration recently published a measurement finding $\mathcal{B}(W \rightarrow e\nu)/\mathcal{B}(W \rightarrow \mu\nu) = 0.9967 \pm 0.0004 \pm 0.0101$ [18], which exceeds the previous ATLAS measurements in precision. All measurements are in good agreement and no evidence of lepton flavour non-universality is observed.

5. – Summary

In these proceedings, the status of lepton flavour universality tests at LHCb was discussed as of *Les Rencontres de Physique de la Vallée d'Aoste 2017*. No hints of lepton flavour non-universality at tree level are seen in $W \rightarrow \ell\nu$ decays, but the LHCb Collaboration finds a tension of 2.1σ in studies of $\bar{B}^0 \rightarrow D^{*+}\tau^-\bar{\nu}_\tau$ decays. Furthermore, a tension of similar size of 2.6σ is observed in $B^+ \rightarrow K^+\ell^+\ell^-$ decays. The latter anomaly is supported by a preliminary LHCb result presented at a recent CERN seminar [19] finding the ratio of $B^0 \rightarrow K^{*0}\ell^+\ell^-$, $R_{K^{*0}}$ to be

$$(6a) \quad R_{K^{*0}} = 0.660_{-0.070}^{+1.10} \pm 0.024 \quad \text{for} \quad 0.045 < q^2 < 1.1 \text{ GeV}^2,$$

$$(6b) \quad R_{K^{*0}} = 0.685_{-0.069}^{+0.113} \pm 0.047 \quad \text{for} \quad 1.1 < q^2 < 6.0 \text{ GeV}^2,$$

corresponding to deviations from the Standard Model of $2.2 - 2.4\sigma$ and of $2.4 - 2.5\sigma$, respectively, depending on the Standard Model calculation. These latest results point in the same direction as R_K and further analyses will shed light onto the nature of these anomalies.

REFERENCES

- [1] LHCb COLLABORATION (AAIJ R. *et al.*), *Phys. Rev. Lett.*, **113** (2014) 151601, arXiv:1406.6482 [hep-ex].
- [2] LHCb COLLABORATION (AAIJ R. *et al.*), *JHEP*, **06** (2014) 133, arXiv:1403.8044 [hep-ex].
- [3] LHCb COLLABORATION (AAIJ R. *et al.*), *JHEP*, **09** (2015) 133, arXiv:1506.08777 [hep-ex].
- [4] LHCb COLLABORATION (AAIJ R. *et al.*), *JHEP*, **06** (2015) 115, arXiv:1503.07138 [hep-ex].
- [5] LHCb COLLABORATION (AAIJ R. *et al.*), *JHEP*, **02** (2016) 104, arXiv:1512.04442 [hep-ex].
- [6] BELLE COLLABORATION (WEHLE S. *et al.*), arXiv:1612.05014 [hep-ex].

- [7] BEČIREVIĆ D., FAJFER S., KOŠNIK N. and SUMENSARI O., *Phys. Rev. D*, **94** (2016) 115021, arXiv:1608.08501 [hep-ph]; CRIVELLIN A., MÜLLER D. and OTA T., arXiv:1703.09226 [hep-ph].
- [8] DESCOTES-GENON S., MATIAS J. and VIRTO J., *Phys. Rev. D*, **88** (2013) 074002, arXiv:1307.5683 [hep-ph]; GAULD R., GOERTZ F. and HAISCH U., *JHEP*, **01** (2014) 069, arXiv:1310.1082 [hep-ph]; BURAS A. J., DE FAZIO F., GIRRBACH J. and CARLUCCI M. V., *JHEP*, **01** (2013) 023, arXiv:1211.1237 [hep-ph]; ALTMANNSHOFER W. and STRAUB D. M., *Phys. Rev. D*, **89** (2014) 095033, arXiv:1403.1269 [hep-ph]; ALTMANNSHOFER W., GORI S., PROFUMO S. and QUEIROZ F. S., *JHEP*, **12** (2016) 106, arXiv:1609.04026 [hep-ph].
- [9] BOBETH C., HILLER G. and OIRANISHVILI G., *JHEP*, **12** (2007) 040, arXiv:0709.4174 [hep-ph]; BORDONE M., ISIDORI G. and PATTORI A., *Eur. Phys. J. C*, **76** (2016) 440, arXiv:1605.07633 [hep-ph].
- [10] BELLE COLLABORATION (WEI J.-T. *et al.*), *Phys. Rev. Lett.*, **103** (2009) 171801, arXiv:0904.0770 [hep-ex].
- [11] BABAR COLLABORATION (LEES J. P. *et al.*), *Phys. Rev. D*, **86** (2012) 032012, arXiv:1204.3933 [hep-ex].
- [12] LHCb COLLABORATION (AAIJ R. *et al.*), *Phys. Rev. Lett.*, **115** (2015) 111803, arXiv:1506.08614 [hep-ex].
- [13] FAJFER S., KAMENIK J. F. and NIŠANDŽIĆ IVAN, *Phys. Rev. D*, **85** (2012) 094025, arXiv:1203.2654 [hep-ph]; AOKI S. *et al.*, arXiv:1607.00299 [hep-lat].
- [14] BABAR COLLABORATION (LEES J. P. *et al.*), *Phys. Rev. Lett.*, **109** (2012) 101802, arXiv:1205.5442 [hep-ex].
- [15] LHCb COLLABORATION (AAIJ R. *et al.*), *JHEP*, **10** (2016) 030, arXiv:1608.01484 [hep-ex].
- [16] LHCb COLLABORATION (AAIJ R. *et al.*), *JHEP*, **01** (2016) 155, arXiv:1511.08039 [hep-ex].
- [17] HFAG (AMHIS Y. *et al.*), arXiv:1612.07233 [hep-ex] and online update at <http://www.slac.stanford.edu/xorg/hfag/>.
- [18] ATLAS COLLABORATION (AABOUD M. *et al.*), arXiv:1612.03016 [hep-ex].
- [19] BIFANI S. on behalf of the LHCb COLLABORATION, <https://indico.cern.ch/event/580620/>.